ImmunoHorizons

RESEARCH ARTICLE

Innate Immunity

A Population of Injury-Responsive Lymphoid Cells Expresses *mpeg1.1* in the Adult Zebrafish Heart

Bethany R. Moyse and Rebecca J. Richardson

School of Physiology, Pharmacology and Neuroscience, Faculty of Life Sciences, University of Bristol, Bristol BS8 1TD, United Kingdom

ABSTRACT

Transgenic zebrafish that express fluorophores under the control of *mpeg1.1* (*mpeg1*) and *csf1ra* (*c-fms*) promoters have been widely used to study the dynamics and functions of mononuclear phagocytes (MNPs) in larval zebrafish, unveiling crucial roles for these innate immune cells in many processes, including tissue repair. Adult zebrafish are also being increasingly used as a model organism for such studies because of their regenerative capacity and presence of innate and adaptive immune cells. For example, recent investigations highlight roles of MNPs in the regulation of diverse cellular processes during heart regeneration, including scarring, cardiomyocyte proliferation, and neovascularization. However, transgenic lines that stratify MNP subpopulations (monocytes, macrophages, and dendritic cells) are not yet available, preventing functional analysis of these populations. In an attempt to better segregate cardiac MNPs, we assessed the coexpression of *mpeg1.1* and *csf1ra* reporter transgenes in adult zebrafish hearts. Unexpectedly, this also identified a discrete population of *mpeg1.1*$^{+}$*csf1ra*$^{-}$ lymphoid-like cells, which respond to cardiac cryoinjury in a different temporal pattern to *mpeg1.1*$^{+}$ MNPs. *mpeg1.1*$^{+}$ lymphoid cells were also abundant in the skin, spleen, and blood, and their frequency was unaffected in the hearts of *csf1ra*$^{j4e1/j4e1}$ mutant zebrafish, which display deficiencies in MNP populations. Flow cytometry, imaging, and cytological and gene expression analyses collectively indicate that these cells comprise a mixed population of B cells and NK-like cells. Our study therefore highlights the need to identify novel MNP lineage markers but also suggests undetermined roles of B cells and NK-like cells in cardiac homeostasis and repair in adult zebrafish. *ImmunoHorizons*, 2020, 4: 464–474.

INTRODUCTION

A correctly balanced and timely inflammatory response is essential to achieve successful repair and regeneration of injured tissue (1–9). As regeneration is inefficient in the majority of adult mammalian tissues, the resultant scar deposition and poor restoration of functional cells is central to the pathology of many diseases (10). This is particularly pertinent following myocardial infarction, in which the incomplete replenishment of cardiomyocytes and chronic scarring can cause an irreversible decline in cardiac function and lead to heart failure (11–13). Understanding the beneficial and harmful interplay between inflammation and tissue repair may therefore provide clues on how to enhance a regenerative response in mammalian tissues. Recent studies in teleost fish, amphibians, and rodents suggest that the recruitment of immune cell populations to sites of tissue injury is more conserved between vertebrates than previously thought, despite apparent differences in regenerative capacity (1, 2, 4, 5, 8). For instance, the recruitment of innate and adaptive immune cells to acute cardiac injury in the highly regenerative adult zebrafish is similar to that observed in nonregenerative rodent models, indicating that subtle differences in inflammatory response may impact regenerative ability (1, 2, 9).

Received for publication July 1, 2020. Accepted for publication July 17, 2020.

Address correspondence and reprint requests to: Dr. Rebecca J. Richardson, C21a, Biomedical Sciences Building, School of Physiology, Pharmacology and Neuroscience, University of Bristol, University Walk, Bristol BS8 1TD, U.K. E-mail address: rebecca.richardson@bristol.ac.uk

ORCIDs: 0000-0003-4434-9194 (B.R.M.); 0000-0002-4701-8713 (R.J.R.).

This work was supported by a British Heart Foundation Intermediate Fellowship (FS/15/2/31225) (to R.J.R.) and a Wellcome Trust–funded Ph.D. studentship (108907/Z/15/Z) (to B.R.M.).

Abbreviations used in this article: *csf1ra*, CSF 1 receptor α; DC, dendritic cell; dpi, day postinjury; FSC, forward scatter; MNP, mononuclear phagocyte; *mpeg1.1*, macrophage expressed 1, tandem duplicate 1; NKL, NK-like; SSC, side scatter.

The online version of this article contains supplemental material.

https://doi.org/10.4049/immunohorizons.2000063

Cells of the mononuclear phagocyte (MNP) system, which comprises monocytes, tissue macrophages, and dendritic cells (DCs) (14, 15), have been a primary focus of tissue repair research, including in the context of cardiac injury, given their involvement in processes such as scarring and neovascularization (1, 3, 5, 6, 8, 9). In humans and rodents, in which MNP lineages are routinely defined by Ab labeling of precise protein markers, the diverse and crucial roles that monocyte and macrophage subpopulations play during repair and regeneration of the heart and other tissues has begun to be characterized (5, 16, 17). However, the recent finding that monocyte and macrophage subtypes play significant roles in mediating the beneficial outcome of cardiac stem cell therapies emphasizes the need to further elucidate the precise mechanisms of MNP activity following tissue injury (18).

Fundamental roles of MNPs in many aspects of development and disease have also been uncovered in larval zebrafish (19). Furthermore, the discovery that zebrafish hematopoiesis is strikingly similar to that of mammalian systems (20–24), including the establishment of a sophisticated adaptive immune system by 3 wk postfertilization, has opened up new avenues of investigation in adult zebrafish (21, 25). The recent characterization of zebrafish T lymphocytes (26), B lymphocytes (20, 27), and innate lymphoid cells such as NK cells (23) has demonstrated that the function and organization of immune cell populations share many similarities to their mammalian counterparts. Combined with their regenerative capacity, the adult zebrafish therefore provides a unique model system to characterize the complex inflammatory processes that govern natural regeneration in vertebrates.

Studies in zebrafish have benefitted from the creation of numerous transgenic lines that permit the visualization, tracking, and downstream investigations of virtually any cell type. This includes the development of macrophage expressed 1, tandem duplicate 1 (*mpeg1.1*, commonly known as *mpeg1*) (28) and CSF 1 receptor α (*csf1ra*, also known as *c-fms*) (29, 30) reporter transgenic lines, which have been repeatedly used to label global macrophage populations, predominantly in larval studies. Recently, we have used these macrophage transgenics, alongside a transgenic reporter for the classical proinflammatory macrophage marker *tnfa*, to show that subpopulations of $tnfa^{+}$ and $tnfa^{-}$ MNPs play different roles in response to cardiac cryoinjury in adult zebrafish (1). However, although *mpeg1.1*- and *csf1ra*-driven transgenes are conventionally reported to label macrophages in the zebrafish, they are likely to label all cells of the MNP system. As alternative genes that specifically label monocyte, macrophage, and DC populations have not yet been established in zebrafish, we cannot yet discern the dynamics of these populations during homeostasis and following injury.

In this study, we aimed to further characterize subpopulations of MNPs in the adult heart by stratifying cells via their coexpression of *mpeg1.1* and *csf1ra*; however, in doing so, we unexpectedly identified a population of lymphoid-like cells resident in the heart that express *mpeg1.1*. Extending our analysis to the blood, spleen, and fin, we show that this population is found consistently within both hematopoietic and functional tissues of the adult zebrafish, confirming a similar recent report describing this in the whole kidney marrow and other tissues of adult zebrafish (31). Additionally, we show that these $mpeg1.1^{+}$ lymphoid cells respond to cardiac cryoinjury in a different temporal manner to *csf1ra*-expressing MNPs. These $mpeg1.1^{+}$ lymphoid cells could be distinguished from $mpeg1.1^{+}$ MNPs by their morphology, granularity, and limited *csf1ra, mfap4*, and *marco* expression. Analysis of *csf1ra* mutant fish also revealed normal numbers of $mpeg1.1^{+}$ lymphoid cells despite deficiencies of MNPs within the heart, further suggesting that Csf1ra is not required for formation, differentiation, or function of these lymphoid cells. Collectively, the data presented in this study supports evidence that *mpeg1.1* marks a population of lymphoid cells as well as MNPs and that this lymphocyte population is expanded following cardiac injury.

MATERIALS AND METHODS

Zebrafish lines and procedures

The Tg(*mpeg1:mCherry*) (28), TgBAC(*csf1ra:GFP*) (29), and $csf1ra^{j4e1/j4e1}$ (32) zebrafish lines have been described previously. Adult fish used were aged 4–18 mo, and fish were randomly chosen from mixed sex tanks housing up to 20 individuals. Animals were anesthetized via immersion in 0.025% MS-222 (A5040; Sigma) in aquarium facility water for all procedures, once for a maximum of 5 min. Animals were euthanized via immersion in an overdose of anesthetic. All lines were maintained according to standard procedures, and all animal work was carried out in accordance with U.K. Home Office and local University of Bristol regulations. Cardiac injuries on adult zebrafish were carried out as described previously (33). Briefly, fish were anesthetized and placed ventral side up in a precut sponge soaked in aquarium water containing anesthetic. A 4-mm incision was made through the skin and the pericardial sac directly above the heart to expose the ventricle. The ventricle was dried using a sterile cotton swab and a liquid nitrogen cooled probe was applied to the exposed ventricle for 30 s.

Imaging

Tissues were dissected and washed in ice-cold PBS, fixed in 4% paraformaldehyde (P6148; Sigma) at 4°C, and then further washed in PBS prior to mounting and imaging. Imaging was performed on a Leica TCS SP8 AOBS confocal laser scanning microscope using a 10×/0.4 HC PL APO Dry or 20×/0.75 HC PL APO CS2 immersion objective. For live imaging of blood circulation, zebrafish were anesthetized and placed on a wetted sponge, and the tail was immobilized with 1% low gelling temperature agarose (A9414; Sigma). Within the heated (28°C) microscope chamber, fish were placed in a reservoir and intubated with flowing (3–4 ml/min) aquarium water containing 0.016% MS-222. Images were acquired using a Leica SP8 multiphoton system using a 25×/0.95 HC Fluotar water dipping lens and resonance scanning at 8000 Hz. Images and videos were processed and brightness was adjusted using Fiji (34).

Tissue preparation for FACS analysis

Heart. The ventricle was dissected, gently torn open, and washed in ice-cold perfusion buffer (10 mM HEPES, 30 mM taurine, and

5.5 mM glucose in PBS). Tissue was digested in perfusion buffer plus 0.25% trypsin, 12.5 μM $CaCl_2$, and 5 mg/ml collagenase II (LS004176; Worthington Biochemical) for up to 2 h at 32°C and agitated at 800 rpm, with regular pipetting to aid digestion. To stop digestion, the cell suspension was placed on ice and mixed with one volume of perfusion buffer plus 10% (v/v) FBS (11591821; Thermo Fisher Scientific) and 12.5 μM $CaCl_2$. Cells were pelleted (1500 rpm, 8 min, 4°C), resuspended in PBS plus 2% FBS and 0.8 μM $CaCl_2$, and filtered through a 40-μm Falcon Cell Strainer (22363547; Thermo Fisher Scientific).

Fin. The caudal fin was excised, gently disaggregated using forceps, and washed in PBS, and a cell suspension was prepared as previously described for the ventricle.

Blood. Immediately following dissection of the heart, 3–10 μl blood filling the chest cavity was collected using a heparin-coated pipette tip, mixed with 10 μl 500 iU/ml heparin (A16198; Alfa Aesar), and then mixed with ice-cold PBS plus 5% FBS (PBS/FBS). Cells were pelleted, resuspended in 750 μl ACK Lysing Buffer (LZ10-548E; SLS), and incubated for 10 min at room temperature with gentle agitation to lyse RBCs. Lysis was terminated by the addition of 750 μl ice-cold PBS/FBS. Cells were pelleted and resuspended in PBS/FBS.

Spleen. Spleens were dissected and mechanically dissociated in PBS/FBS by gently passing the tissue through a 40-μm cell strainer. RBCs were lysed, and the cell suspension was prepared as previously described for blood.

FACS analysis

All cells were kept on ice until analysis. Immediately prior to sorting, DRAQ7 (ab109202; Abcam) was added to the cell suspension to stain dead cells. Flow cytometry analysis and FACS was carried out at 4°C using a BD Influx Fluorescence Associated Cell Sorter. For sorting and analysis, events were gated to select single, live cells (see Supplemental Fig. 1 for gating strategy). Cells were sorted into a 1.5 ml Eppendorf containing PBS. FCS files generated from sorts were analyzed using FlowJo_v10.6.2 software.

Cytology

FACS-sorted cells were resuspended in 200 μl PBS and spun (1000 rpm, 5 min) onto a microscope slide using a Cytospin Cytocentrifuge (Thermo Fisher Scientific). Slides were dried and fixed in methanol for 5 min, stained in May–Grünwald stain for 5 min, then transferred to Giemsa stain for 10 min. Slides were rinsed in 3.3 mM Sorenson buffer (pH 6.8) for 3 min to differentiate and then left to dry. Cytospins were imaged on an Olympus BX53 Upright Microscope with a ×40 objective. Cell measurements were performed manually on Fiji by measuring the longest diameter of the cell body, excluding protrusions.

RNA extraction and RT-PCR

RNA extraction was performed from sorted cells using TRI Reagent (T9424; Sigma) and Phasemaker Tubes (A33248; Invitrogen), according to the manufacturer's instructions. RNA concentration was determined by 260/280 absorption ratios using a NanoDrop 2000 Spectrophotometer (Thermo Fisher Scientific). RNA was reverse transcribed using a Maxima H Minus First Strand cDNA Synthesis Kit (K1682; Thermo Fisher Scientific), according to the manufacturer's instructions. Target genes were amplified (40 cycles) from cDNA using the primers listed in Supplemental Table I with a QIAGEN Fast Cycling PCR Kit (203745), according to the manufacturer's instructions, on a Bio-Rad T100 Thermal Cycler machine.

Statistics

In all cases, *n* numbers refer to biological replicates unless otherwise stated; where pools of ventricles were used, this is stated in the figure/legend. Raw data recording and analysis was conducted using GraphPad Prism 8.2.1. Statistical significance was determined via nonparametric Mann–Whitney or Kruskal–Wallis/Dunn multiple comparison tests or parametric ANOVA (details provided in figure legends). In all cases, error bars represent SD. For all datasets, a Grubb outlier test was performed, and any significant outliers ($\alpha = 0.05$) were removed. Asterisks represent statistical significance ($^*p < 0.05$, $^{**}p < 0.01$, $^{***}p < 0.005$).

RESULTS

Imaging and flow cytometry identify a population of mpeg1.1$^+$ lymphoid-like cells in the heart

We have recently characterized the recruitment of different inflammatory cell populations to the heart following cardiac cryoinjury in adult zebrafish and shown that macrophage subtypes are required for proper scar deposition and subsequent resolution during regeneration (1). To investigate cardiac macrophage subtype dynamics further, we examined Tg(*mpeg1.1:mCherry*); TgBAC(*csf1ra:GFP*) double-transgenic fish in more detail (Fig. 1). When examining macrophage populations in the ventricle and atrium of Tg(*mpeg1.1:mCherry*); TgBAC(*csf1ra:GFP*) double-transgenic fish via confocal microscopy, we observed a small but consistent population of *mpeg1.1:mCherry* expressing cells, which lacked *csf1ra:GFP* expression (Fig. 1A, 1B), denoted *mpeg1.1*$^+$ cells. These *mpeg1.1*$^+$ cells generally appeared rounded and small (arrowheads in Fig. 1B) in comparison with double-positive *mpeg1.1*$^+$*csf1ra*$^+$ cells that appeared larger and more stellate, typical of mature, tissue-resident MNPs.

Consistent with these findings, flow cytometry of cells isolated from the ventricles of Tg(*mpeg1.1:mCherry*); TgBAC(*csf1ra:GFP*) double-transgenic fish also revealed that although the majority (71.0% ± 6.3% SD) of labeled cells expressed both fluorophores, 18% ± 6.7% SD of labeled cells were *mpeg1.1*$^+$ (Fig. 1C, Supplemental Fig. 2A). A minority of cells also appeared *mpeg1.1*$^-$*csf1ra*$^+$ (*csf1ra*$^+$; 1.2% ± 0.8% SD; Fig. 1C, Supplemental Fig. 2A). Forward scatter (FSC) and side scatter (SSC), indicative of cell size and granularity, respectively, also show that *mpeg1.1*$^+$ cells are small and have a low granularity unlike the *mpeg1.1*$^+$*csf1ra*$^+$ population (Fig. 1D), which was confirmed by cytological analysis of these populations (Fig. 1E, 1F). A distinct lymphocyte-like

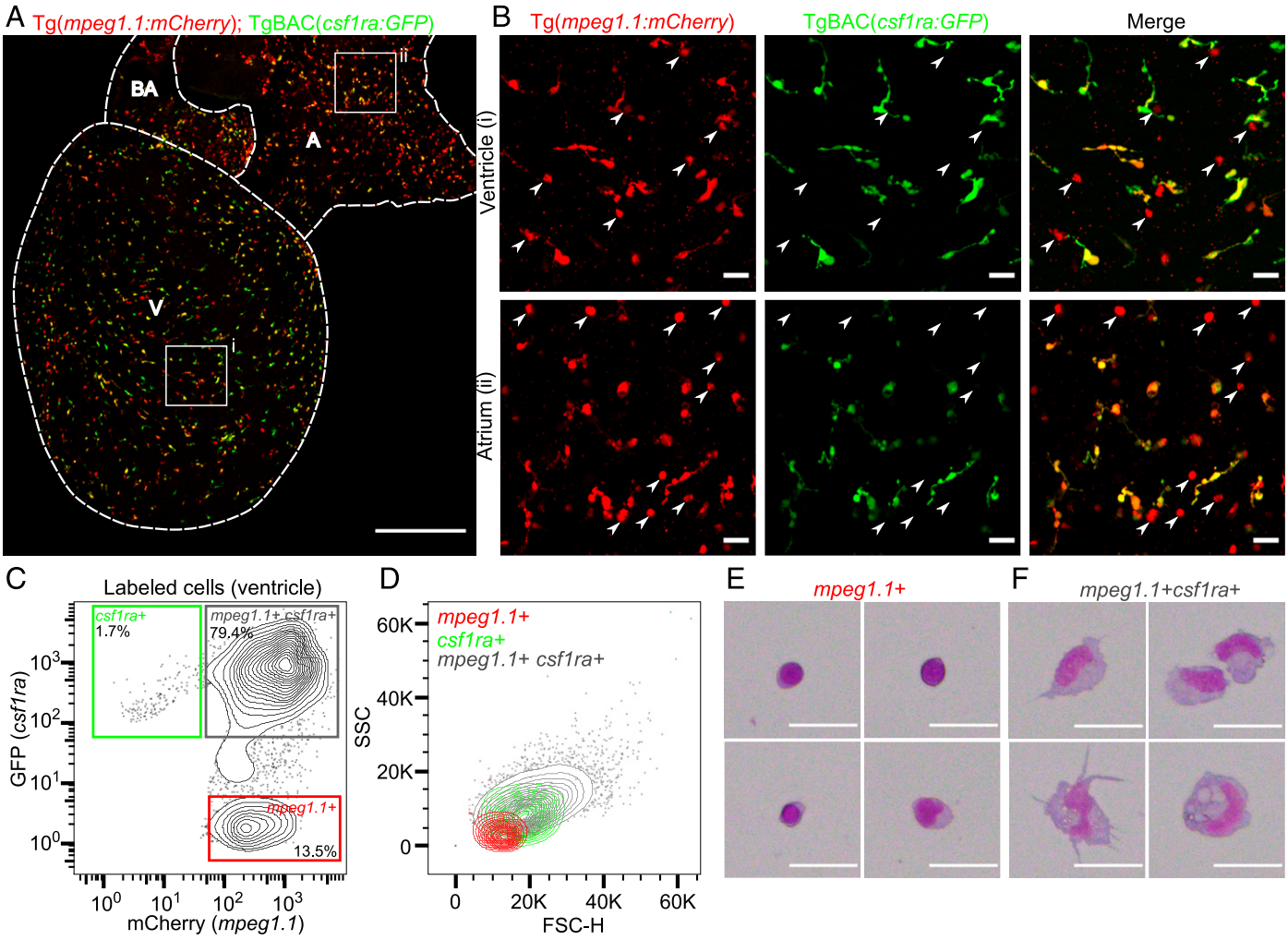

FIGURE 1. A distinct population of *mpeg1.1:mCherry*$^+$ cells exist in adult Tg(*mpeg1.1:mCherry*); TgBAC(*csf1ra:GFP*) zebrafish hearts.
(**A**) Whole-mount image of an adult Tg(*mpeg1.1:mCherry*); TgBAC(*csf1ra:GFP*) zebrafish heart. Outlined regions identify the ventricle (V), atrium (A), and bulbus arteriosus (BA). (**B**) Higher magnification imaging of labeled cells within the ventricle (i) and atrium (ii) identified by the insets in (A). Arrowheads identify cells that express *mpeg1.1:mCherry* but lack *csf1ra:GFP* expression (*mpeg1.1*$^+$ cells). (**C** and **D**) Flow cytometric analysis of Tg(*mpeg1.1:mCherry*); TgBAC(*csf1ra:GFP*) adult zebrafish ventricles. Representative plots from two pooled ventricles. (C) GFP and mCherry reporter expression in labeled cells showing gating for single- and double-positive populations. (D) FSC and SSC analysis of *mpeg1.1*$^+$, *csf1ra*$^+$, and *mpeg1.1*$^+$*csf1ra*$^+$ populations identified in (C). (**E** and **F**) Representative examples of May–Grünwald Giemsa–stained cytospin preparations of *mpeg1.1*$^+$ and *mpeg1.1*$^+$*csf1ra*$^+$ cells isolated by FACS. One experimental replicate of six pooled ventricles. Scale bars, (A) 300 μm, (B, E, and F) 20 μm.

appearance was observed in the majority of *mpeg1.1*$^+$ cells (Fig. 1E) with an average cell body diameter of 8.1 ± 2.4 μm SD (Supplemental Fig. 2B). In contrast, *mpeg1.1*$^+$*csf1ra*$^+$ cells resembled monocytes, macrophages, and DCs (Fig. 1F); cells appeared larger (average diameter = 18.0 ± 4.0 μm SD; Supplemental Fig. 2B) and had a low nuclear to cytoplasmic ratio, and many cells were vacuolated and/or had many protrusions (15, 35, 36).

mpeg1.1$^+$ *lymphoid cells are present in other adult tissues*

Next, we sought to determine the distribution of *mpeg1.1*$^+$ lymphoid-like cells in other tissues of adult zebrafish (Fig. 2). Confocal imaging in the spleen (Fig. 2A), vasculature (Fig. 2B, Supplemental Video 1), and fins (Fig. 2C) of Tg(*mpeg1.1:mCherry*); TgBAC(*csf1ra:GFP*) adult zebrafish revealed *mpeg1.1*$^+$, *mpeg1.1*$^+$*csf1ra*$^+$, and *csf1ra*$^+$ cells in all tissues analyzed. As observed in the ventricle, *mpeg1.1*$^+$ cells presented with a smaller and more rounded morphology compared with *csf1ra:GFP*-expressing cells, although this was seen to a lesser extent within fin tissue (Fig. 2A–C). The discrete *mpeg1.1*$^+$ population was also identifiable in the spleen, whole blood, and caudal fin by flow cytometry, consistently presenting with lower *mCherry* expression and forward and SSC characteristics compared with the *mpeg1.1*$^+$*csf1ra*$^+$ cells (Fig. 2D–F, Supplemental Fig. 2C–E). Interestingly, each tissue displayed a unique distribution of *mpeg1.1* and *csf1ra* transgene expression (Fig. 2D–F) yet the *mpeg1.1*$^+$

https://doi.org/10.4049/immunohorizons.2000063

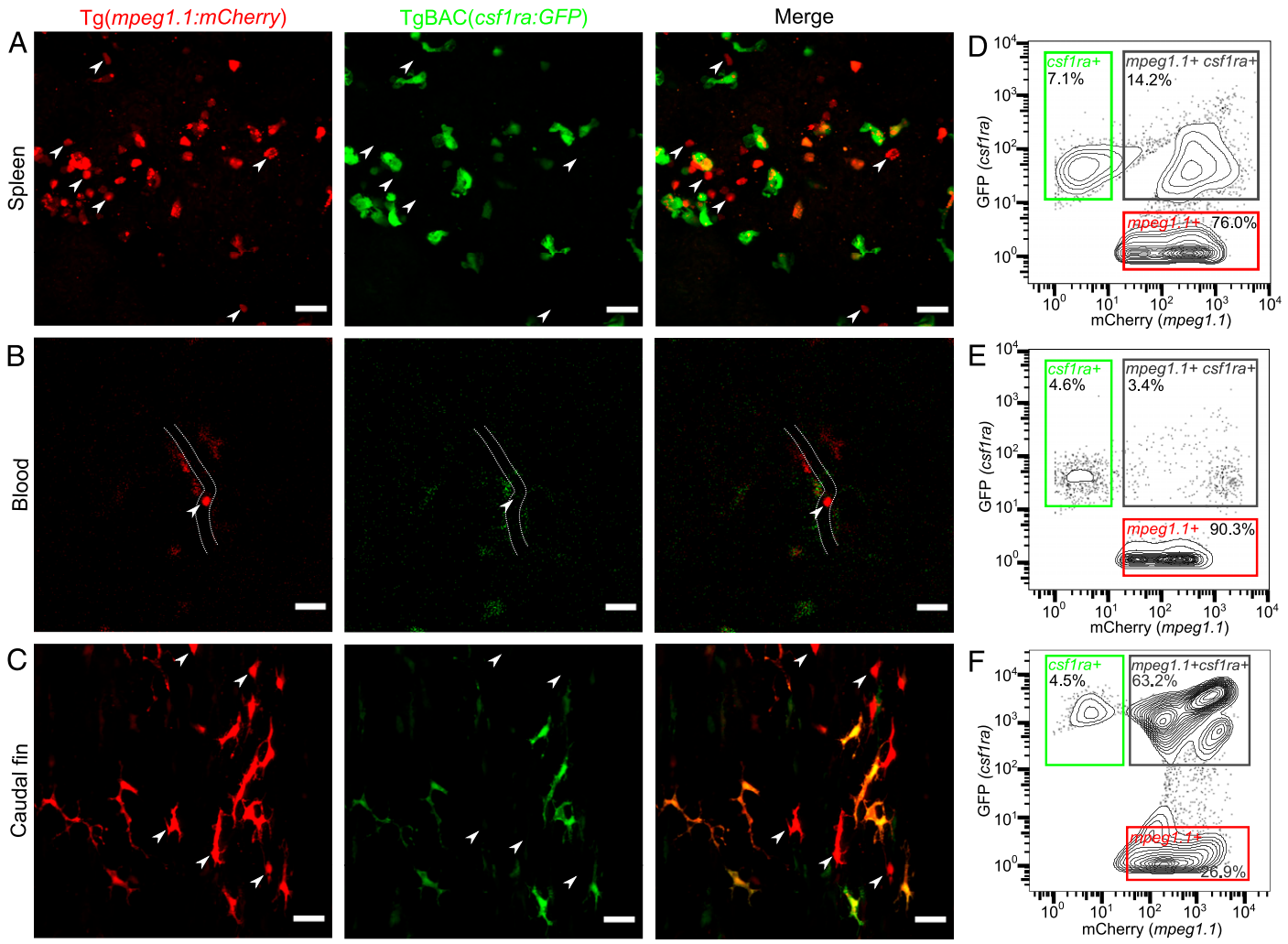

FIGURE 2. *mpeg1.1*$^+$ lymphoid-like cells are found in the spleen, blood, and caudal fin of adult Tg(*mpeg1.1:mCherry*); TgBAC(*csf1ra:GFP*) zebrafish.

(**A**–**C**) Confocal imaging in the spleen (A), circulation (B), and caudal fin (C). Arrowheads identify *mpeg1.1*$^+$ cells. (A and C) Whole-mount imaging in fixed tissues. (B) Single frame from live imaging of the circulation (see Supplemental Video 1). Dotted white line outlines the vessel through which an *mpeg1.1*$^+$ cell is traveling. (**D**–**F**) Representative plots of flow cytometry analysis of the spleen (D), blood (E), and caudal fin (F). Scale bars, (A–C) 20 μm.

population comprised a large proportion of labeled cells within the spleen and blood (76.0% [single experiment of pool of five samples]; 85.7% ± 5.2% SD [n = 5], respectively).

Cytospin preparations of *mpeg1.1*$^+$ cells from the caudal fin also revealed a similar lymphoid appearance in the majority of cells, although larger, rounded cells resembling plasma cells and mature macrophages were also present (Supplemental Fig. 2F). Alongside the observations made by imaging and flow cytometry analysis (Fig. 2C, 2F), this may suggest that *mpeg1.1* is expressed in an additional *csf1ra*-negative population unique to the skin/fin. Indeed, the morphology of these cells is similar to that of the recently described nonmyeloid cell type, metaphocytes, which perform Ag processing functions in the skin of adult zebrafish (37, 38). Therefore, our data suggest that two populations of *mpeg1.1*$^+$ cells that do not express *csf1ra* exist in adult skin. As expected, the *mpeg1.1*$^+$*csf1ra*$^+$ fin cells resembled a mixed population of MNPs (Supplemental Fig. 2E–G). It is also worth noting that whereas the FSC/SSC profile of *csf1ra*$^+$ cells in the heart, blood, and spleen was characteristic of myeloid cells, *csf1ra*$^+$ cells in the fin possessed a very high SSC (Supplemental Fig. 2E). This is likely due to the inclusion of xanthophores, pigment-producing cells of the skin, which are also known to express *csf1ra* (32, 39).

mpeg1.1$^+$ lymphoid cells respond to cardiac injury

Our data demonstrate that *mpeg1.1*$^+$ lymphoid-like cells are present in the heart and other tissues of adult zebrafish during homeostasis. To determine if and how these cells respond to injury, we performed cardiac cryoinjury on adult Tg(*mpeg1.1:mCherry*); TgBAC(*csf1ra:GFP*)

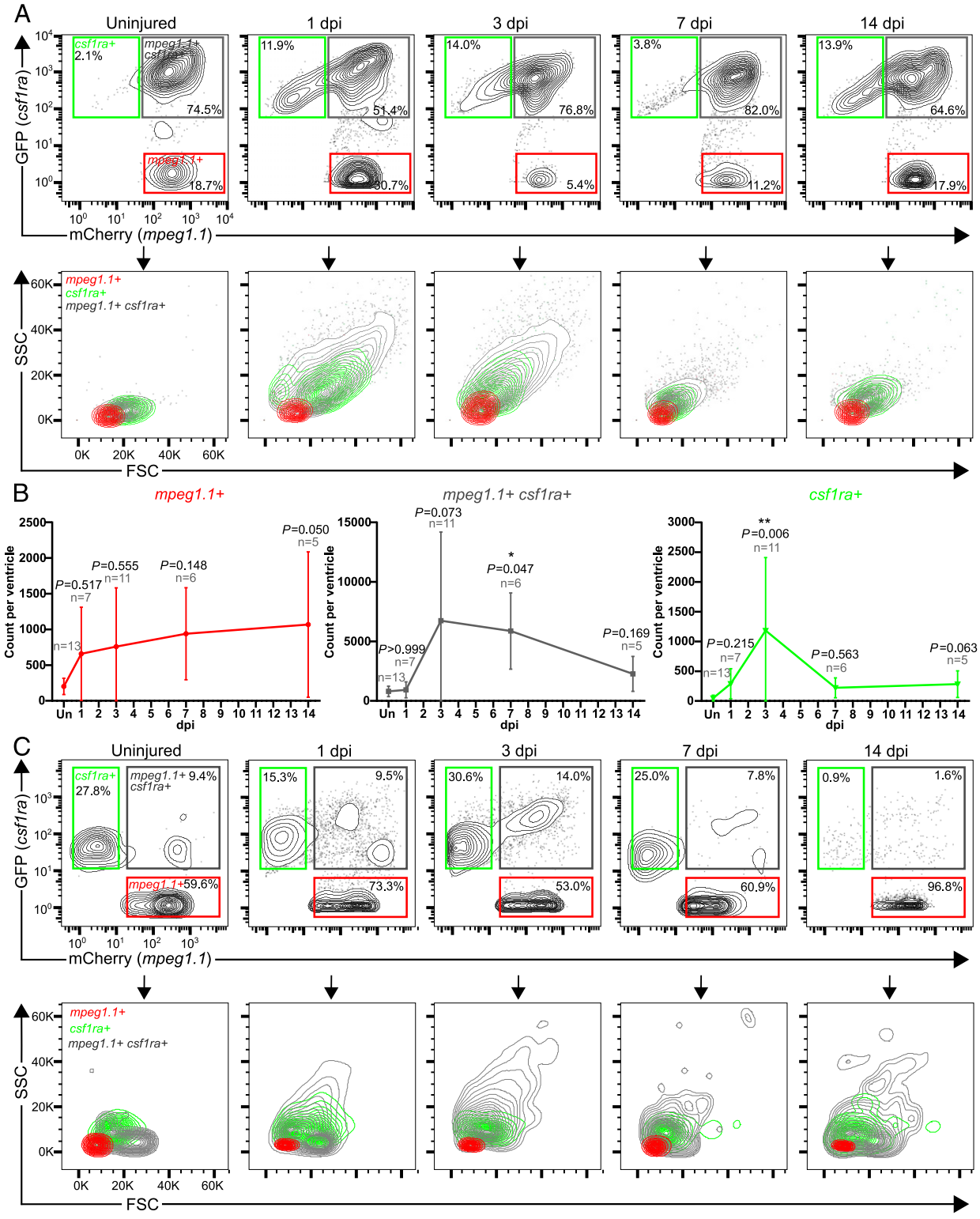

FIGURE 3. *mpeg1.1*$^+$ cells are responsive to cardiac injury.

(**A**–**C**) Flow cytometry analysis of ventricular tissue and whole blood isolated from Tg(*mpeg1.1:mCherry*); TgBAC(*csf1ra:GFP*) zebrafish at key timepoints following cardiac cryoinjury. (A) Exemplar plots and relative percentages of *mpeg1.1:mCherry* and *csf1ra:GFP* reporter fluorescence intensity of labeled cells isolated from ventricular tissue at the specified timepoints (top) with the corresponding forward and SSC profiles of the subpopulations shown below. (B) Mean ± SD frequency of each cell population expressed as the total cell count per ventricle. Two independent experiments. Statistical analysis was performed by Kruskal–Wallis with Dunn multiple comparison tests; *p* values are timepoint **(Continued)**

https://doi.org/10.4049/immunohorizons.2000063

zebrafish and harvested ventricular tissue and whole blood at 1, 3, 7, and 14 d postinjury (dpi; Fig. 3) for flow cytometric analysis. In line with our previous observations (1), an accumulation of MNPs (*mpeg1.1*$^+$*csf1ra*$^+$) was observed within the ventricle at 3 and 7 dpi (Fig. 3A, top, 3B) and showed increased size and granularity at 1 and 3 dpi (Fig. 3A, bottom), likely because of the activation of these cells, which is expected in the early phases of tissue repair. Similarly, the frequency and FSC/SSC characteristics of the *csf1ra*$^+$ cells peaked within 1 wk postinjury (Fig. 3B). The increased FSC and SSC of *mpeg1.1*$^+$*csf1ra*$^+$ and *csf1ra*$^+$ populations following injury was also mirrored in the blood (Fig. 3C); however, frequencies of the subpopulations could not be quantified because of high variability (data not shown). The fluorescence distribution, FSC/SSC profile, and dynamics of the *csf1ra*-expressing populations suggests that they include monocytes, which are mobilized to the blood and recruited to the ventricular tissue within the first week postinjury. However, unlike the transient expansion of the *csf1ra*-expressing populations, the frequency of *mpeg1.1*$^+$ cells within the ventricle increased throughout the time course, and cells remained small and nongranular in both the ventricle and blood, further supporting their lymphoid origin (Fig. 3).

Collectively, this confirms that *csf1ra*$^+$ and *mpeg1.1*$^+$*csf1ra*$^+$ populations within the heart and blood respond to cardiac injury with the expected dynamics of MNPs, whereas the number of *mpeg1.1*$^+$ lymphoid cells is expanded at later stages of repair and remains elevated in the heart for longer.

The mpeg1.1$^+$ *cells in adult tissues express markers of B cells and NK-like cells*

mpeg1.1 expression has been previously reported in B cell and NK-like (NKL) cells isolated from the whole kidney marrow of adult zebrafish by a single-cell transcriptomic approach (22). To further dissect the identity of the *mpeg1.1*$^+$ lymphoid-like population, we therefore assessed the *mpeg1.1*$^{\pm}$*csf1ra*$^{\pm}$ subpopulations for the expression of monocyte/macrophage, B cell, and NKL cell lineage markers by RT-PCR (Fig. 4). This analysis was performed on cells sorted from whole blood at 3 dpi to obtain large numbers of cells for each population and to avoid collection of the proposed nonlymphoid cells within the *mpeg1.1*$^+$ population, which were identified in the fin (Fig. 2).

As expected, *mpeg1.1*$^+$*csf1ra*$^+$ and *csf1ra*$^+$ cells showed clear expression of *csf1ra*, *mpeg1.1*, *mpeg1.2*, *mfap4*, and *marco*, which are reported to show monocyte/macrophage-associated expression in zebrafish (40). Endogenous expression of *mpeg1.1* in *csf1ra*$^+$ cells, which show low *mpeg1.1:mCherry* reporter expression, further suggests that *csf1ra*$^+$ cells in the blood are immature monocytes that could be transitioning into mature *mpeg1.1*$^+$*csf1ra*$^+$ MNPs and likely reflects the delay in mCherry fluorophore synthesis, although

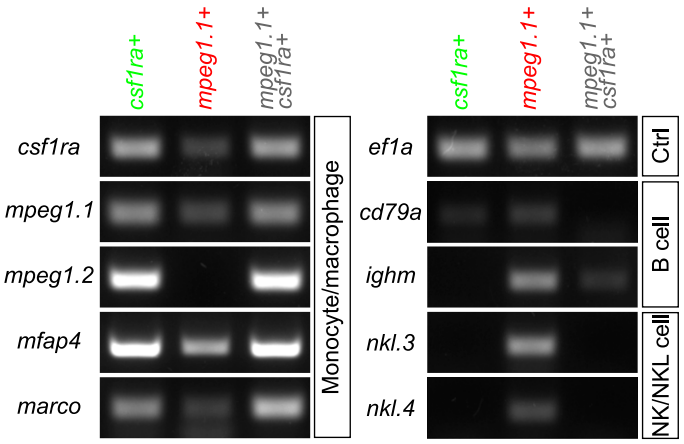

FIGURE 4. *mpeg1.1*$^+$ cells express B cell– and NKL cell–specific transcripts.

RT-PCR of mRNA isolated from *mpeg1.1*$^{\pm}$*csf1ra*$^{\pm}$ cell populations sorted from whole blood at 3 d post–cardiac cryoinjury to determine the expression of monocyte/macrophage, B cell, and NK/NKL cell transcripts. *ef1a* was used as a control (Ctrl).

we cannot completely rule out contamination between populations (Fig. 4). In contrast, *mpeg1.1*$^+$ cells demonstrated low expression of monocyte/macrophage genes yet showed distinct expression of B cell– (*cd79a* and *ighm*) (27) and NKL cell (*nkl.3* and *nkl.4*) (22)–associated genes, which were absent in both *csf1ra*-expressing populations (Fig. 4). This analysis therefore further supports the identity of *mpeg1.1*$^+$*csf1ra*$^+$ and *csf1ra*$^+$ cells as MNPs and indicates that the *mpeg1.1*$^+$ population comprise a mixed population of B cells and NKL cells.

mpeg1.1$^+$ *lymphoid cell populations are normal in csf1ra*$^{j4e1/j4e1}$ *zebrafish*

To further confirm that the *mpeg1.1*$^+$ population identifies cells of a nonmyeloid origin, we compared the relative frequency of *mpeg1.1*$^{\pm}$*csf1ra*$^{\pm}$ subpopulations in the ventricle of adult zebrafish, which have a loss of function mutation in *csf1ra* (*csf1ra*$^{j4e1/j4e1}$ or *panther* mutants) (32). Like rodents, *csf1ra* mutant zebrafish exhibit reduced numbers of MNPs because of the critical role of Csf1r in normal MNP differentiation, proliferation, and survival (14, 41–45). We therefore proposed that *mpeg1.1*$^+$ populations should be minimally affected in *csf1ra*$^{j4e1/j4e1}$ zebrafish, whereas *csf1ra*-expressing populations should be drastically reduced.

Indeed, imaging of the uninjured ventricle of wildtype and *csf1ra*$^{j4e1/j4e1}$; Tg(*mpeg1.1:mCherry*) transgenic zebrafish showed that *csf1ra*$^{j4e1/j4e1}$ mutants have sparse *mpeg1.1:mCherry*-labeled cells within the ventricle unlike wildtype controls (Fig. 5A). Many of the remaining cells appeared to have a lymphocyte-like morphology

compared with uninjured controls; and asterisks identify statistically significant values. (C) Exemplar plots of *mpeg1.1:mCherry* and *csf1ra:GFP* reporter fluorescence intensity of labeled cells isolated from whole blood at the specified timepoints (top) with the corresponding forward and SSC profiles of the subpopulations shown below. One independent experiment. *n*, number of fish per timepoint; Un, uninjured.

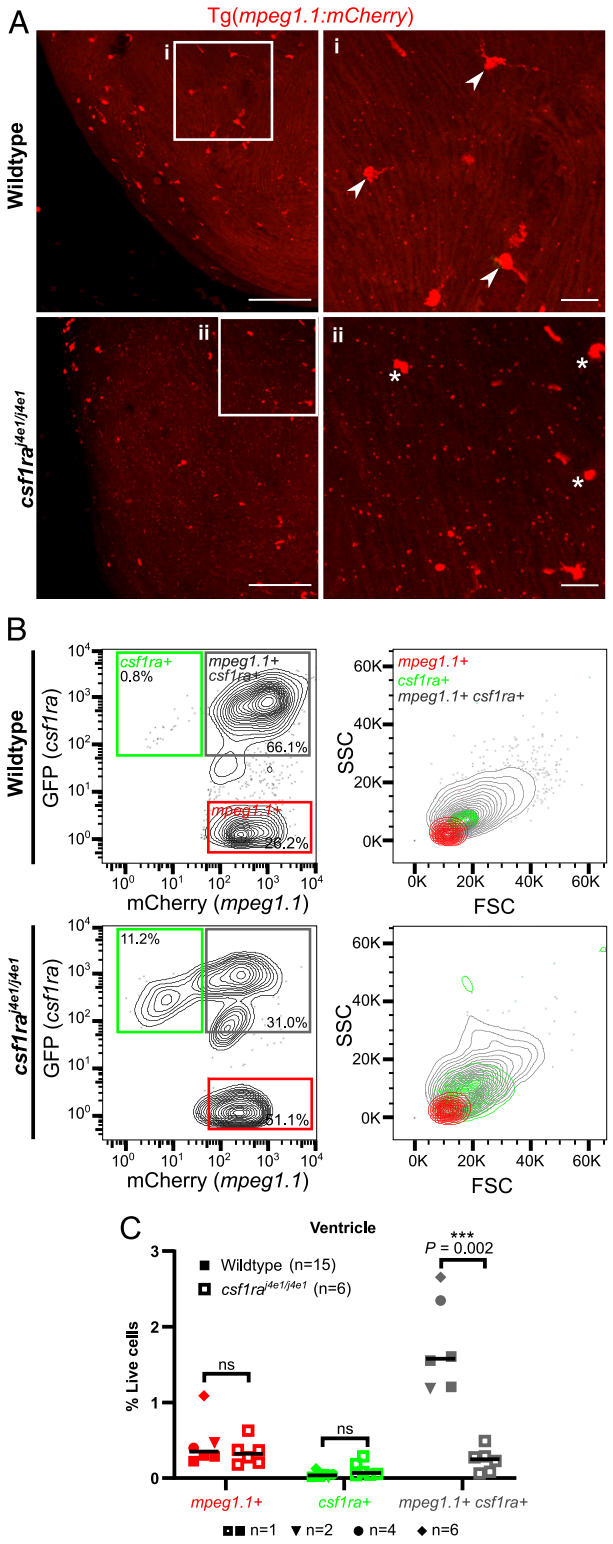

FIGURE 5. *csf1ra*$^{j4e1/j4e1}$ zebrafish have reduced numbers of MNPs but normal *mpeg1.1*$^{+}$ lymphoid cells.

(**A**) Whole-mount imaging of Tg(*mpeg1.1:mCherry*) fluorescence in the ventricle of uninjured wildtype and *csf1ra*$^{j4e1/j4e1}$ adult zebrafish. Right images (i and ii) correspond to the regions identified within the left images. Images show that fluorescent cells are sparse and have a smaller, more rounded morphology in *csf1ra*$^{j4e1/j4e1}$ (asterisks) compared with wildtype controls (arrowheads indicate larger, more protrusive macrophages). (**B** and **C**) Flow cytometric analysis of wildtype and *csf1ra*$^{j4e1/j4e1}$; Tg(*mpeg1.1:mCherry*); TgBAC(*csf1ra:GFP*) uninjured, adult ventricles. (B) Exemplar plots of *mpeg1.1:mCherry* and *csf1ra:GFP* expression of labeled cells (left) and the associated forward and SSC profile of the cell populations (right) in wildtype and *csf1ra*$^{j4e1/j4e1}$ adult zebrafish ventricles. Single ventricle for each condition. (C) Frequency of cell populations in wildtype and *csf1ra*$^{j4e1/j4e1}$ Tg(*mpeg1.1:mCherry*); Tg(*csf1ra:GFP*) zebrafish as a percentage of live, single cells. Key indicates number of ventricles in pooled experiments. Statistical analysis performed by Mann–Whitney *U* test. Scale bars, left, 100 μm; right, 20 μm.

as previously described for *mpeg1.1*$^{+}$ cells in wildtype (Fig. 5A). Flow cytometry of uninjured ventricles from *csf1ra*$^{j4e1/j4e1}$; Tg(*mpeg1.1:mCherry*); Tg(*csf1ra:GFP*) adult fish confirmed that *mpeg1.1*$^{+}$, *mpeg1.1*$^{+}$*csf1ra*$^{+}$, and *csf1ra*$^{+}$ populations are still present; however, *mpeg1.1*$^{+}$ cells make up a larger proportion of the labeled cells compared with wildtype ventricles (Fig. 5B). Comparing the frequency of these populations between wildtype and *csf1ra* mutant zebrafish ventricles showed that, as proposed, there is a significant reduction in *mpeg1.1*$^{+}$*csf1ra*$^{+}$ MNPs (p = 0.0022); however, the *mpeg1.1*$^{+}$ and *csf1ra*$^{+}$ populations appeared normal (Fig. 5C).

DISCUSSION

The genetic tractability, live-cell imaging capabilities, and presence of many mammalian orthologs has led to the creation of hundreds of transgenic zebrafish lines, which has facilitated the study of many diverse cell types (15, 28–30, 46–49). These advantages have been extensively used to explore the dynamics of cells of the MNP system, primarily macrophages, and has led to many important discoveries about the development and function of these cells during homeostasis and disease. However, the heterogeneity and unique tissue-specific development of MNPs complicate the study of these cells, and thus far, only a handful of transgenic markers that label these populations have been developed. Detailed comparisons of zebrafish and mammalian immune systems is therefore required and will simultaneously provide insights into how the inflammatory response can facilitate regeneration in adult tissue.

To better define monocyte and macrophage populations within the adult zebrafish heart during homeostasis and following injury, we have assessed the expression of two classically used promoters to drive expression in macrophages in zebrafish, *mpeg1.1*, and *csf1ra*. *Csf1r* (also known as *fms*) is a classical macrophage marker in mammals (41, 42). The identification of two zebrafish orthologs of *csf1r*, *csf1ra* and *csf1rb*, and their conserved expression within MNPs led to the creation of *csf1ra* reporter transgenics (29, 30). However, additional expression of *csf1ra* in neural crest-derived cells has compromised their usefulness in tracking MNPs

in isolation in the zebrafish (32). Many studies have therefore used *mpeg1.1*, historically referred to as *mpeg1*, to label macrophage populations. Validation studies performed in larval zebrafish showed that endogenous and transgene-derived *mpeg1.1* is exclusively expressed in primitive and definitive macrophages and is coexpressed with *csf1r* (28, 40), making it a valuable tool to specifically study macrophage dynamics in vivo, which was not previously possible. However, as transgene expression is sustained throughout adulthood (28), multiple studies have since used *mpeg1.1* transgenics to study macrophages in adult zebrafish without thorough validation of its reporter specificity. In this study, we have therefore characterized the expression of *mpeg1.1* and *csf1ra* in adult zebrafish tissues, with a particular focus on the heart. We show that the vast majority of labeled cells in the uninjured heart highly express both transgenes (71.0% ± 6.3% SD), likely representing mature tissue-resident macrophages. Additionally, we identified a small population of cells in all tissues examined, including the blood, that appear to strongly express *csf1ra* but express undetectable or low levels of *mpeg1.1*, suggesting these could be a population of monocytes.

Our finding that *mpeg1.1*-driven transgenes are expressed in additional populations of non-MNP cells in the heart, blood, and other tissues of adult zebrafish confirms recent reports that *mpeg1.1* is not exclusively a macrophage-specific marker in adult zebrafish (22, 31). In accordance with a recent report (31), we also show that *mpeg1.1*$^+$ lymphoid cells express markers of *ighm*$^+$ B cells, and their distinct lymphocyte-like morphology and abundance in hematopoietic tissues supports this finding (36, 50). However, we also provide new evidence that *mpeg1.1*$^+$ cells harness a transcriptional profile of NKL cells. The presence of NK and NKL cells in zebrafish has been determined by the identification of orthologs of mammalian NK-specific genes, namely novel immune-type receptors and NK lysins, by single-cell sequencing and morphological studies (22, 23, 51, 52). However, functional studies of these cells have not yet been performed. *mpeg1.1* transgenics may therefore aid the characterization of these elusive cells. Our data also support the recent description of *mpeg1.1*$^+$ epidermal metaphocytes (37, 38), suggesting additional markers will be required to stratify these *mpeg1.1*$^+$*csf1ra*$^-$ populations in studies in the skin.

The expansion of the putative *mpeg1.1*$^+$ B cells and NKL cells following cardiac injury (Fig. 3) also warrants future investigation as studies in mammalian models suggest that these cells have active roles in heart repair. Importantly for our investigation into the roles of MNPs in zebrafish heart regeneration, mature B cells have been shown to mediate monocyte recruitment and detrimental inflammatory-mediated tissue dysfunction in the heart (53, 54). Similarly, NK cells have been shown to affect monocyte maturation during inflammation and have also been linked with beneficial angiogenic and fibrotic responses in mammals (55–57).

Among others, our study highlights the need to identify novel markers of monocyte, macrophage, and DC subpopulations to facilitate more detailed investigation of these cells in larval and adult zebrafish. Determining the reporter specificity of *mfap4* transgenics in adult zebrafish, which has not yet been well reported, may aid these studies (48). Nevertheless, we show that by combining *csf1ra* and *mpeg1.1* transgenics, the specificity of labeling of MNPs can be improved by excluding contaminating lymphoid cells and pigment cells that express *mpeg1.1* and *csf1ra*, respectively. This also prevents the need to segregate cells by size and granularity characteristics, which may not be possible in all tissues and may exclude rare populations of cells. This study also raises questions about the function of *mpeg1.1* and its paralogues *mpeg1.2* and *mpeg1.3* in zebrafish immunology, which have been described to have distinct roles and be expressed at different stages of zebrafish development (58). Furthermore, as we observed a complete lack of *mpeg1.2* expression within the *mpeg1.1*$^+$ lymphoid population (Fig. 4), the lineage specificity of *mpeg1.2* expression in adult zebrafish requires further characterization.

In summary, our study has further dissected the dynamics of MNP populations within the heart during homeostasis and throughout the initial phases in heart repair and regeneration. Simultaneously, we have confirmed that *mpeg1.1* is expressed by B cells, provided new evidence for *mpeg1.1* expression in NKL cells, and proposed the involvement of these cells following injury. This highlights the need to further characterize and diversify the use of transgenic reporters in adult zebrafish. Continued in-depth characterization of precise inflammatory populations, via gene expression profiling, careful flow cytometry evaluations, and live imaging, in regenerative models such as zebrafish will allow new insights into the precise roles these cell types play in the regenerative response, harnessing the unique power of zebrafish as a model organism.

DISCLOSURES

The authors have no financial conflicts of interest.

ACKNOWLEDGMENTS

We thank the Wolfson Bioimaging Facility for imaging expertise, Andrew Herman, Lorena Sueiro Ballesteros, and Helen Rice for cell sorting in the University of Bristol Faculty of Biomedical Sciences Flow Cytometry Facility, and the laboratory of Prof. Jan Frayne (School of Biochemistry, University of Bristol) for assistance with cytology.

REFERENCES

1. Bevan, L., Z. W. Lim, B. Venkatesh, P. R. Riley, P. Martin, and R. J. Richardson. 2020. Specific macrophage populations promote both cardiac scar deposition and subsequent resolution in adult zebrafish. *Cardiovasc. Res.* 116: 1357–1371.
2. Hui, S. P., D. Z. Sheng, K. Sugimoto, A. Gonzalez-Rajal, S. Nakagawa, D. Hesselson, and K. Kikuchi. 2017. Zebrafish regulatory T cells mediate organ-specific regenerative programs. *Dev. Cell* 43: 659–672.e5.
3. Godwin, J. W., A. R. Pinto, and N. A. Rosenthal. 2013. Macrophages are required for adult salamander limb regeneration. *Proc. Natl. Acad. Sci. USA* 110: 9415–9420.
4. Aurora, A. B., E. R. Porrello, W. Tan, A. I. Mahmoud, J. A. Hill, R. Bassel-Duby, H. A. Sadek, and E. N. Olson. 2014. Macrophages are

required for neonatal heart regeneration. *J. Clin. Invest.* 124: 1382–1392.
5. Lavine, K. J., S. Epelman, K. Uchida, K. J. Weber, C. G. Nichols, J. D. Schilling, D. M. Ornitz, G. J. Randolph, and D. L. Mann. 2014. Distinct macrophage lineages contribute to disparate patterns of cardiac recovery and remodeling in the neonatal and adult heart. [Published erratum appears in 2016 Proc. Natl. Acad. Sci. USA 113: E1414.] *Proc. Natl. Acad. Sci. USA* 111: 16029–16034.
6. de Preux Charles, A. S., T. Bise, F. Baier, J. Marro, and A. Jaźwińska. 2016. Distinct effects of inflammation on preconditioning and regeneration of the adult zebrafish heart. *Open Biol.* 6: 160102.
7. Sattler, S., and N. Rosenthal. 2016. The neonate versus adult mammalian immune system in cardiac repair and regeneration. *Biochim. Biophys. Acta* 1863(7 Pt B): 1813–1821.
8. Godwin, J. W., R. Debuque, E. Salimova, and N. A. Rosenthal. 2017. Heart regeneration in the salamander relies on macrophage-mediated control of fibroblast activation and the extracellular landscape. *NPJ Regen. Med.* 2: 22.
9. Lai, S. L., R. Marín-Juez, P. L. Moura, C. Kuenne, J. K. H. Lai, A. T. Tsedeke, S. Guenther, M. Looso, and D. Y. Stainier. 2017. Reciprocal analyses in zebrafish and medaka reveal that harnessing the immune response promotes cardiac regeneration. *eLife* 6: e25605.
10. Ueha, S., F. H. Shand, and K. Matsushima. 2012. Cellular and molecular mechanisms of chronic inflammation-associated organ fibrosis. *Front. Immunol.* 3: 71.
11. Uygur, A., and R. T. Lee. 2016. Mechanisms of cardiac regeneration. *Dev. Cell* 36: 362–374.
12. Talman, V., and H. Ruskoaho. 2016. Cardiac fibrosis in myocardial infarction-from repair and remodeling to regeneration. *Cell Tissue Res.* 365: 563–581.
13. Prabhu, S. D., and N. G. Frangogiannis. 2016. The biological basis for cardiac repair after myocardial infarction: from inflammation to fibrosis. *Circ. Res.* 119: 91–112.
14. Hume, D. A. 2006. The mononuclear phagocyte system. *Curr. Opin. Immunol.* 18: 49–53.
15. Wittamer, V., J. Y. Bertrand, P. W. Gutschow, and D. Traver. 2011. Characterization of the mononuclear phagocyte system in zebrafish. *Blood* 117: 7126–7135.
16. Novak, M. L., and T. J. Koh. 2013. Macrophage phenotypes during tissue repair. *J. Leukoc. Biol.* 93: 875–881.
17. Das, A., M. Sinha, S. Datta, M. Abas, S. Chaffee, C. K. Sen, and S. Roy. 2015. Monocyte and macrophage plasticity in tissue repair and regeneration. *Am. J. Pathol.* 185: 2596–2606.
18. Vagnozzi, R. J., M. Maillet, M. A. Sargent, H. Khalil, A. K. Z. Johansen, J. A. Schwanekamp, A. J. York, V. Huang, M. Nahrendorf, S. Sadayappan, and J. D. Molkentin. 2020. An acute immune response underlies the benefit of cardiac stem cell therapy. *Nature* 577: 405–409.
19. Morales, R. A., and M. L. Allende. 2019. Peripheral macrophages promote tissue regeneration in zebrafish by fine-tuning the inflammatory response. *Front. Immunol.* 10: 253.
20. Page, D. M., V. Wittamer, J. Y. Bertrand, K. L. Lewis, D. N. Pratt, N. Delgado, S. E. Schale, C. McGue, B. H. Jacobsen, A. Doty, et al. 2013. An evolutionarily conserved program of B-cell development and activation in zebrafish. *Blood* 122: e1–e11.
21. Stachura, D. L., and D. Traver. 2016. Cellular dissection of zebrafish hematopoiesis. *Methods Cell Biol.* 133: 11–53.
22. Tang, Q., S. Iyer, R. Lobbardi, J. C. Moore, H. Chen, C. Lareau, C. Hebert, M. L. Shaw, C. Neftel, M. L. Suva, et al. 2017. Dissecting hematopoietic and renal cell heterogeneity in adult zebrafish at single-cell resolution using RNA sequencing. *J. Exp. Med.* 214: 2875–2887.
23. Hernández, P. P., P. M. Strzelecka, E. I. Athanasiadis, D. Hall, A. F. Robalo, C. M. Collins, P. Boudinot, J. P. Levraud, and A. Cvejic. 2018. Single-cell transcriptional analysis reveals ILC-like cells in zebrafish. *Sci. Immunol.* 3: eaau5265.
24. Davidson, A. J., and L. I. Zon. 2004. The 'definitive' (and 'primitive') guide to zebrafish hematopoiesis. *Oncogene* 23: 7233–7246.
25. Gore, A. V., L. M. Pillay, M. Venero Galanternik, and B. M. Weinstein. 2018. The zebrafish: a fintastic model for hematopoietic development and disease. *Wiley Interdiscip. Rev. Dev. Biol.* 7: e312.
26. Langenau, D. M., A. A. Ferrando, D. Traver, J. L. Kutok, J. P. Hezel, J. P. Kanki, L. I. Zon, A. T. Look, and N. S. Trede. 2004. In vivo tracking of T cell development, ablation, and engraftment in transgenic zebrafish. *Proc. Natl. Acad. Sci. USA* 101: 7369–7374.
27. Liu, X., Y. S. Li, S. A. Shinton, J. Rhodes, L. Tang, H. Feng, C. A. Jette, A. T. Look, K. Hayakawa, and R. R. Hardy. 2017. Zebrafish B cell development without a pre-B cell stage, revealed by CD79 fluorescence reporter transgenes. *J. Immunol.* 199: 1706–1715.
28. Ellett, F., L. Pase, J. W. Hayman, A. Andrianopoulos, and G. J. Lieschke. 2011. mpeg1 promoter transgenes direct macrophage-lineage expression in zebrafish. *Blood* 117: e49–e56.
29. Dee, C. T., R. T. Nagaraju, E. I. Athanasiadis, C. Gray, L. Fernandez Del Ama, S. A. Johnston, C. J. Secombes, A. Cvejic, and A. F. Hurlstone. 2016. CD4-transgenic zebrafish reveal tissue-resident Th2- and regulatory T cell-like populations and diverse mononuclear phagocytes. *J. Immunol.* 197: 3520–3530.
30. Gray, C., C. A. Loynes, M. K. Whyte, D. C. Crossman, S. A. Renshaw, and T. J. Chico. 2011. Simultaneous intravital imaging of macrophage and neutrophil behaviour during inflammation using a novel transgenic zebrafish. *Thromb. Haemost.* 105: 811–819.
31. Ferrero, G., E. Gomez, S. Lyer, M. Rovira, M. Miserocchi, D. M. Langenau, J. Y. Bertrand, and V. Wittamer. 2020. The macrophage-expressed gene (mpeg) 1 identifies a subpopulation of B cells in the adult zebrafish. *J. Leukoc. Biol.* 107: 431–443.
32. Parichy, D. M., D. G. Ransom, B. Paw, L. I. Zon, and S. L. Johnson. 2000. An orthologue of the kit-related gene fms is required for development of neural crest-derived xanthophores and a subpopulation of adult melanocytes in the zebrafish, *Danio rerio*. *Development* 127: 3031–3044.
33. González-Rosa, J. M., and N. Mercader. 2012. Cryoinjury as a myocardial infarction model for the study of cardiac regeneration in the zebrafish. *Nat. Protoc.* 7: 782–788.
34. Schindelin, J., I. Arganda-Carreras, E. Frise, V. Kaynig, M. Longair, T. Pietzsch, S. Preibisch, C. Rueden, S. Saalfeld, B. Schmid, et al. 2012. Fiji: an open-source platform for biological-image analysis. *Nat. Methods* 9: 676–682.
35. Lugo-Villarino, G., K. M. Balla, D. L. Stachura, K. Bañuelos, M. B. Werneck, and D. Traver. 2010. Identification of dendritic antigen-presenting cells in the zebrafish. *Proc. Natl. Acad. Sci. USA* 107: 15850–15855.
36. Traver, D., B. H. Paw, K. D. Poss, W. T. Penberthy, S. Lin, and L. I. Zon. 2003. Transplantation and in vivo imaging of multilineage engraftment in zebrafish bloodless mutants. *Nat. Immunol.* 4: 1238–1246.
37. Lin, X., Q. Zhou, C. Zhao, G. Lin, J. Xu, and Z. Wen. 2019. An ectoderm-derived myeloid-like cell population functions as antigen transporters for langerhans cells in zebrafish epidermis. *Dev. Cell* 49: 605–617.e5.
38. Kuil, L. E., N. Oosterhof, G. Ferrero, T. Mikulášová, M. Hason, J. Dekker, M. Rovira, H. C. van der Linde, P. M. van Strien, E. de Pater, et al. 2020. Zebrafish macrophage developmental arrest underlies depletion of microglia and reveals Csf1r-independent metaphocytes. *eLife* 9: e53403.
39. Parichy, D. M., and J. M. Turner. 2003. Temporal and cellular requirements for Fms signaling during zebrafish adult pigment pattern development. *Development* 130: 817–833.
40. Zakrzewska, A., C. Cui, O. W. Stockhammer, E. L. Benard, H. P. Spaink, and A. H. Meijer. 2010. Macrophage-specific gene functions in Spi1-directed innate immunity. *Blood* 116: e1–e11.

41. Stanley, E. R., D. M. Chen, and H. S. Lin. 1978. Induction of macrophage production and proliferation by a purified colony stimulating factor. *Nature* 274: 168–170.
42. Stanley, E. R., L. J. Guilbert, R. J. Tushinski, and S. H. Bartelmez. 1983. CSF-1–a mononuclear phagocyte lineage-specific hemopoietic growth factor. *J. Cell. Biochem.* 21: 151–159.
43. Cecchini, M. G., M. G. Dominguez, S. Mocci, A. Wetterwald, R. Felix, H. Fleisch, O. Chisholm, W. Hofstetter, J. W. Pollard, and E. R. Stanley. 1994. Role of colony stimulating factor-1 in the establishment and regulation of tissue macrophages during postnatal development of the mouse. *Development* 120: 1357–1372.
44. Tushinski, R. J., I. T. Oliver, L. J. Guilbert, P. W. Tynan, J. R. Warner, and E. R. Stanley. 1982. Survival of mononuclear phagocytes depends on a lineage-specific growth factor that the differentiated cells selectively destroy. *Cell* 28: 71–81.
45. Dai, X.-M., G. R. Ryan, A. J. Hapel, M. G. Dominguez, R. G. Russell, S. Kapp, V. Sylvestre, and E. R. Stanley. 2002. Targeted disruption of the mouse colony-stimulating factor 1 receptor gene results in osteopetrosis, mononuclear phagocyte deficiency, increased primitive progenitor cell frequencies, and reproductive defects. *Blood* 99: 111–120.
46. Mathias, J. R., B. J. Perrin, T. X. Liu, J. Kanki, A. T. Look, and A. Huttenlocher. 2006. Resolution of inflammation by retrograde chemotaxis of neutrophils in transgenic zebrafish. *J. Leukoc. Biol.* 80: 1281–1288.
47. Renshaw, S. A., C. A. Loynes, D. M. Trushell, S. Elworthy, P. W. Ingham, and M. K. Whyte. 2006. A transgenic zebrafish model of neutrophilic inflammation. *Blood* 108: 3976–3978.
48. Walton, E. M., M. R. Cronan, R. W. Beerman, and D. M. Tobin. 2015. The macrophage-specific promoter mfap4 allows live, long-term analysis of macrophage behavior during mycobacterial infection in zebrafish. *PLoS One* 10: e0138949.
49. Martins, R. R., P. S. Ellis, R. B. MacDonald, R. J. Richardson, and C. M. Henriques. 2019. Resident immunity in tissue repair and maintenance: the zebrafish model coming of age. *Front. Cell Dev. Biol.* 7: 12.
50. Petrie-Hanson, L., C. Hohn, and L. Hanson. 2009. Characterization of rag1 mutant zebrafish leukocytes. *BMC Immunol.* 10: 8.
51. Moss, L. D., M. M. Monette, L. Jaso-Friedmann, J. H. Leary III., S. T. Dougan, T. Krunkosky, and D. L. Evans. 2009. Identification of phagocytic cells, NK-like cytotoxic cell activity and the production of cellular exudates in the coelomic cavity of adult zebrafish. *Dev. Comp. Immunol.* 33: 1077–1087.
52. Moore, F. E., E. G. Garcia, R. Lobbardi, E. Jain, Q. Tang, J. C. Moore, M. Cortes, A. Molodtsov, M. Kasheta, C. C. Luo, et al. 2016. Single-cell transcriptional analysis of normal, aberrant, and malignant hematopoiesis in zebrafish. *J. Exp. Med.* 213: 979–992.
53. Zouggari, Y., H. Ait-Oufella, P. Bonnin, T. Simon, A. P. Sage, C. Guérin, J. Vilar, G. Caligiuri, D. Tsiantoulas, L. Laurans, et al. 2013. B lymphocytes trigger monocyte mobilization and impair heart function after acute myocardial infarction. *Nat. Med.* 19: 1273–1280.
54. Adamo, L., L. J. Staloch, C. Rocha-Resende, S. J. Matkovich, W. Jiang, G. Bajpai, C. J. Weinheimer, A. Kovacs, J. D. Schilling, P. M. Barger, et al. 2018. Modulation of subsets of cardiac B lymphocytes improves cardiac function after acute injury. *JCI Insight* 3: e120137.
55. Ayach, B. B., M. Yoshimitsu, F. Dawood, M. Sun, S. Arab, M. Chen, K. Higuchi, C. Siatskas, P. Lee, H. Lim, et al. 2006. Stem cell factor receptor induces progenitor and natural killer cell-mediated cardiac survival and repair after myocardial infarction. *Proc. Natl. Acad. Sci. USA* 103: 2304–2309.
56. Ong, S., D. L. Ligons, J. G. Barin, L. Wu, M. V. Talor, N. Diny, J. A. Fontes, E. Gebremariam, D. A. Kass, N. R. Rose, and D. Čiháková. 2015. Natural killer cells limit cardiac inflammation and fibrosis by halting eosinophil infiltration. *Am. J. Pathol.* 185: 847–861.
57. Ong, S., N. R. Rose, and D. Čiháková. 2017. Natural killer cells in inflammatory heart disease. *Clin. Immunol.* 175: 26–33.
58. Benard, E. L., P. I. Racz, J. Rougeot, A. E. Nezhinsky, F. J. Verbeek, H. P. Spaink, and A. H. Meijer. 2015. Macrophage-expressed perforins mpeg1 and mpeg1.2 have an anti-bacterial function in zebrafish. *J. Innate Immun.* 7: 136–152.